

Molecular changes underlying decay of sensory responses and enhanced seizure propensity in peritumoral neurons

Elena Tantillo, Marta Scalera, Elisa De Santis, Nicolò Meneghetti^o, Chiara Cerri, Michele Menicagli, Alberto Mazzoni, Mario Costa, Chiara Maria Mazzanti, Eleonora Vannini^o, and Matteo Caleo

All author affiliations are listed at the end of the article

Corresponding Authors: Eleonora Vannini, PhD, CNR Neuroscience Institute, via G Moruzzi 1, 56124 Pisa (eleonora.vannini@in.cnr.it); Matteo Caleo, PhD, University of Padua, via G. Colombo 3, Italy (matteo.caleo@unipd.it)

Abstract

Background. Glioblastoma growth impacts on the structure and physiology of peritumoral neuronal networks, altering the activity of pyramidal neurons which drives further tumor progression. It is therefore of paramount importance to identify glioma-induced changes in pyramidal neurons, since they represent a key therapeutic target.

Methods. We longitudinally monitored visual evoked potentials after the orthotopic implant of murine glioma cells into the mouse occipital cortex. With laser microdissection, we analyzed layer II-III pyramidal neurons molecular profile and with local field potentials recordings we evaluated the propensity to seizures in glioma-bearing animals with respect to control mice.

Results. We determine the time course of neuronal dysfunction of glioma-bearing mice and we identify a symptomatic stage, based on the decay of visual response. At that time point, we microdissect layer II-III pyramidal neurons and evaluate the expression of a panel of genes involved in synaptic transmission and neuronal excitability. Compared to the control group, peritumoral neurons show a decrease in the expression of the SNARE complex gene SNAP25 and the alpha1 subunit of the GABA-A receptor. No significant changes are detected in glutamatergic (ie, AMPA or NMDA receptor subunit) markers. Further reduction of GABA-A signaling by delivery of a benzodiazepine inverse agonist, DMCM (methyl-6,7-dimethoxy-4-ethyl-beta-carboline-3-carboxylate) precipitates seizures in 2 mouse models of tumor-bearing mice.

Conclusions. These studies reveal novel molecular changes that occur in the principal cells of the tumor-adjacent zone. These modifications may be therapeutically targeted to ameliorate patients' quality of life.

Key Points

1. Glioma-bearing mice have a slowing down of cortical activity and an enhancement of delta wave power.
2. Glioma-bearing mice show a decrease in SNAP25 and in GABA-A alpha1 subunit expression.
3. Glioma-bearing mice are more prone to develop seizures after DMCM administration.

Much evidence has shown that glioma cells cause changes in neural peritumoral tissue. For instance, glioma cells influence neighboring neurons by causing disabling peritumoral dysfunctions¹ and extruding a high amount of glutamate, which results in excitotoxicity and tumor invasion.^{2,3} Glioma cells also potently perturb the dendritic architecture of neurons in the tumor-adjacent zone.⁴

Epileptic seizures, hyperexcitability, and cognitive impairments are the most frequent clinical manifestations of these peritumoral neuronal dysfunctions. In high-grade gliomas, approximately 30%-62% of the patients display seizures which occur predominantly during the onset of the disease⁵ and are often refractory to antiepileptic treatments.⁶ In addition to excess glutamate release,⁷ other factors contribute

Importance of the Study

This study reveals alterations in sensory-driven responses and ongoing cortical oscillations (specifically, a slowing down of activity with an enhancement of the delta wave power) during glioma progression in mice. These parameters may represent novel non-invasive biomarkers to be used for monitoring progression/response to therapy and in prognostic applications. Second, laser-capture microdissection of peritumoral pyramidal neurons at a symptomatic stage is employed for the study of a panel of genes involved in synaptic

transmission and neuronal excitability. We find significant decreases in the expression of the SNARE complex gene SNAP25 and the alpha1 subunit of the GABA-A receptor in principal neurons. An acute, further pharmacological reduction of GABA-A receptor signaling triggers seizure activity in glioma-bearing mice. Altogether, these studies reveal novel players in the complex landscape of glioma-neuron interactions which may represent therapeutic targets for preventing neuronal dysfunctions.

to the hyperexcitability of peritumoral tissue. Indeed, infiltrating glioma cells alter chloride homeostasis which may lead to a switch of gamma-aminobutyric acid (GABA) signaling towards excitation.^{8–10} Peritumoral regions show a significant loss of approximately 35% of GABAergic interneurons, together with a reduction in their firing rates and in the density of their synapses with pyramidal neurons.^{8,10–12} Moreover, perineuronal nets (PNNs), that surround fast-spiking interneurons are degraded by glioma-released proteases and this reduces the firing rate of the surviving peritumoral inhibitory cells.¹⁰ All these events contribute to establishing an unbalanced neuronal network that ultimately leads to enhanced seizure propensity.^{7,13}

A key concept that emerged in the last years is that neuronal activity in pyramidal neurons promotes glioma progression via various mechanisms. Anatomical and electrophysiological evidence has demonstrated neuron-to-glioma glutamatergic synapses, and genetic or pharmacological perturbation of these synaptic contacts slowed down tumor proliferation and invasion in mouse models. Glutamatergic neuronal activity also drives tumor growth via the release of soluble factors, including neuropilin-3, brain-derived neurotrophic factor, and GRP78.^{14,15} Thus, a vicious cycle ensues in which glioma growth causes enhanced activity and this in turn promotes tumor progression.¹⁴

In this scenario, it appears critical to identify glioma-induced changes in the molecular composition of pyramidal neurons, with specific attention to the genes involved in neuronal excitability, as these may represent therapeutic targets.

As the molecular armamentarium of pyramidal neurons may evolve along glioma progression, here we used a longitudinal approach to monitor peritumoral dysfunctions in the tumor-adjacent zone and examined gene-expression patterns in pyramidal neurons at a symptomatic stage. Specifically, we implanted GL261 glioma cells into the occipital cortex of adult mice and followed chronically visual evoked potentials and ongoing cortical oscillations until a decay of sensory response was observed. At this stage, layer II-III pyramidal neurons were microdissected to examine the expression of a panel of genes involved in neuronal excitability.

Methods

Animals and Glioma Induction

Adult (age > postnatal day 60) wild-type C57BL/6J mice bred in our animal facility and housed in a 12 hours light/dark cycle, with food and water available *ad libitum* were used in the experiments. All experimental procedures conformed to the European Communities Council Directive #86/609/EEC were approved by the Italian Ministry of Health (260/2016-PR, released on 11/03/2016). The murine glioma GL261 or CT-2A cells were grown as described¹⁶ in [Supplementary Material](#).

Chronic Electrode Implantation and VEP Recordings

To longitudinally record the neural response of the visual cortex, in both C57BL/6J control ($n = 4$), GL261-bearing ($n = 5$), and CT-2A-bearing ($n = 6$) mice a chronic bipolar electrode was assembled (according to Cerri et al., 2016) and implanted 3 mm lateral to the midline, in correspondence with lambda and at a depth of 0.75 mm from dura. During the surgery, a metal post was also placed on the occipital bone of animals to allow the recording of visually evoked potentials in awake head-fixed mice.¹⁷ After the recovery from the surgery and a period of habituation to the apparatus, awake head-fixed animals were subjected to recording sessions 3 times a week (ie, from day 8 after tumor implantation ([Figure 1A](#))).

Spectral Analysis

To detect power spectra alterations between glioma-bearing and control mice, we analyzed the local field potentials (LFPs) recorded with a blank stimulus during VEP recording sessions. The power spectrum density of LFP signals was estimated by using the Welch method of averaging modified periodograms^{18,19} in a Matlab code.

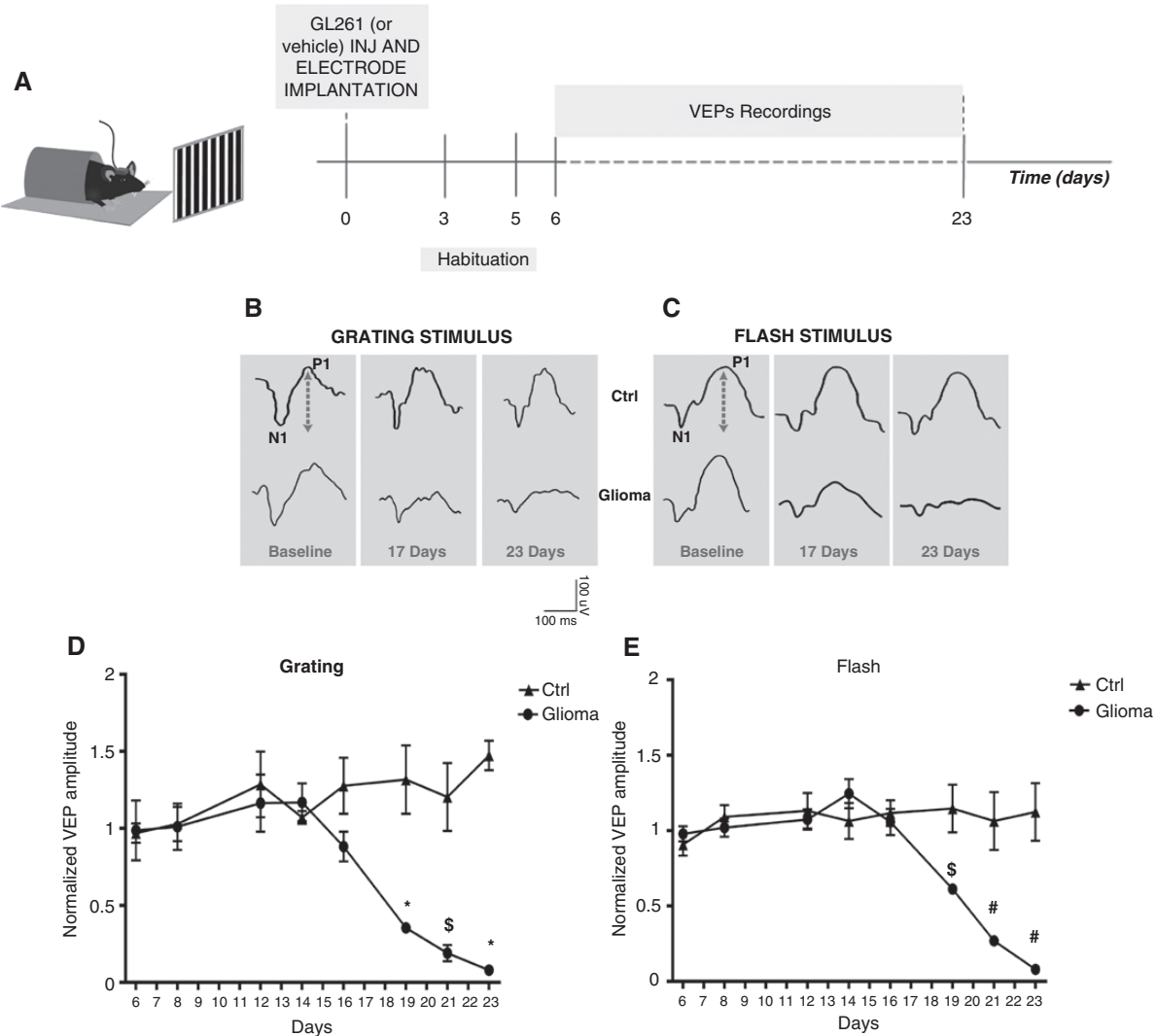


Figure 1. Deterioration of visual responsiveness in glioma-bearing mice along with glioma progression. **(A)** On the left is representative image of a head-fixed mouse during a VEP recording session. On the right is experimental protocol. **(B, C)** Representative VEP waveforms in response to grating (left) and flash (right) stimuli are reported at day 12 (second recording session), 16 (early deterioration), and 23 (last recording sessions) after tumor (Glioma) or PBS (Ctrl) injection. During each recording session, the peak-to-through amplitude of VEP (ie, the N1-P1 amplitude; dotted arrows) was analyzed. N1 indicates the first negative and P1 is the first positive peak of VEP. **(D, E)** Normalized average of VEP amplitude for glioma-bearing (red; $n = 5$) and control (blue; $n = 4$) mice. The mean \pm sem is also shown for each time point. When not visible, error bars are within the symbol (Two-way ANOVA followed by Holm-Sidak test, $P < .05$, $* P < .001$, $\# P < .0001$). The baseline was defined for each type of stimulus averaging the VEP amplitude of the first three recording sessions and each value was normalized on it.

Immunohistochemistry for Laser-capture Microdissection

Extracted brains were gently removed, cryoprotected by immersion in 30% sucrose, and flash-frozen to preserve the RNA integrity. After, a NeuN immunostaining was performed. To further avoid RNA degradation, a fast immunostaining protocol was designed.^{20,21} SuperFrost Plus slides (Thermo Scientific, USA) were sterilized under UV for at least 1 hour. Frozen brains were cut using a cryostat (Leica, Germany) to obtain coronal sections of 7 μm of thickness and slides were immediately placed in a sterile box in dry ice or stored at -80°C until use. At the beginning of immunostaining, slides were kept at room temperature for 10 minutes and

then, incubated for 30 minutes at room temperature in a blocking solution (BSA 10%, Triton-X 1%, PBS); then, slices were incubated for 1 hour room temperature with NeuN primary antibody (1:100, Guinea pig, Synaptic Systems) and 1 hour with anti-guinea pig secondary antibody conjugated to AlexaFluor555 fluorophore (1:200, Thermo Fisher). Slides were washed 2 times in PBS, incubated for 1 min with Hoechst, washed with ddH₂O, and left to dry.^{20,22,23}

Laser-capture Microdissection

Slices were observed with a Zeiss Axio Observer microscope equipped with Zeiss AxioCam MRm camera (Carl

Zeiss MicroImaging GmbH, Germany). For each brain section, the border of the tumor mass was identified with PALMRobo 4.5 Pro program (Zeiss) based on nuclear density through Hoechst staining. Pyramidal neurons of the layers II-III within 500 μm from the tumor rim were selected²⁴ according to cell morphology. Targeted neurons of each mouse were dissected through PALM RoboMover Automatic Laser-capture Microdissector (Zeiss) and collected in separate tubes (Figure 3B) immediately placed in dry ice or at -80°C until processing.

cDNA Synthesis, Preamplification Reaction, and Gene-expression Analysis

A real-time PCR of selected genes (Supplementary Table 1) was performed using SsoAdvanced™ Universal SYBR® Green Supermix (Bio-Rad Laboratories, Hercules, CA), (Bio-Rad Laboratories, USA). The relative expression was calculated using the Livak (DDCt) method and normalized on reference genes (ie, GAPDH and β actin).

Immunohistochemistry and Images Acquisition

A group of vehicle-injected (controls; $n = 6$), GL261-bearing mice ($n = 5$), and CT-2A-bearing mice ($n = 5$) was dedicated to confirming the alterations detected with gene-expression analysis through immunofluorescence staining. Animals were transcardially perfused at 23 (GL261) and at 15 (CT-2A) days, post-injection and extracted brains were cut using a sliding microtome (Leica, Germany) to obtain coronal sections of 50 μm of thickness. Only brains with a visible tumor mass were considered. Sections were stained for GABA α 1 receptor (1:400, Merck, Germany) and SNAP25 (1:1000, Stenberger). Subsequently, they were incubated with fluorophore-conjugated secondary antibodies (Jackson ImmunoResearch, USA) and with Hoechst dye (1:500; Bisbenzamide, Sigma Aldrich, USA) for nuclei visualization.

LFP Recordings and DMCM Administration

A group of vehicle-injected (controls; $n = 5$), GL261-bearing ($n = 4$), and CT-2A-bearing ($n = 6$) mice were specifically devoted to the recording of LFPs in freely moving conditions. A bipolar electrode was implanted in the primary visual cortex as previously described. Signals were acquired by a miniature head stage (NPI, Germany) connected to an amplifier (EXT-02F, NPI). After a period of habituation to the apparatus, animals were recorded for 1-2 h daily starting from days 8 to 11 after tumor implantation. CT-2A-bearing animals received an intraperitoneal injection of saline or DMCM starting from day 11 after tumor induction until day 18. GL261-bearing animals were intraperitoneally injected with saline or DMCM on days 26 and 27, respectively. Control animals received an intraperitoneal injection of saline or DMCM from day 11 to day 18 and then, again, on days 26 and 27. DMCM (methyl-6,7-dimethoxy-4-ethyl-beta-carboline-3-carboxylate) was administered at a sub-convulsive dose (1.5 mg/kg).²⁵ All animals were daily recorded 1 hour before the injection to establish a baseline and 1 hour after saline or DMCM administration.

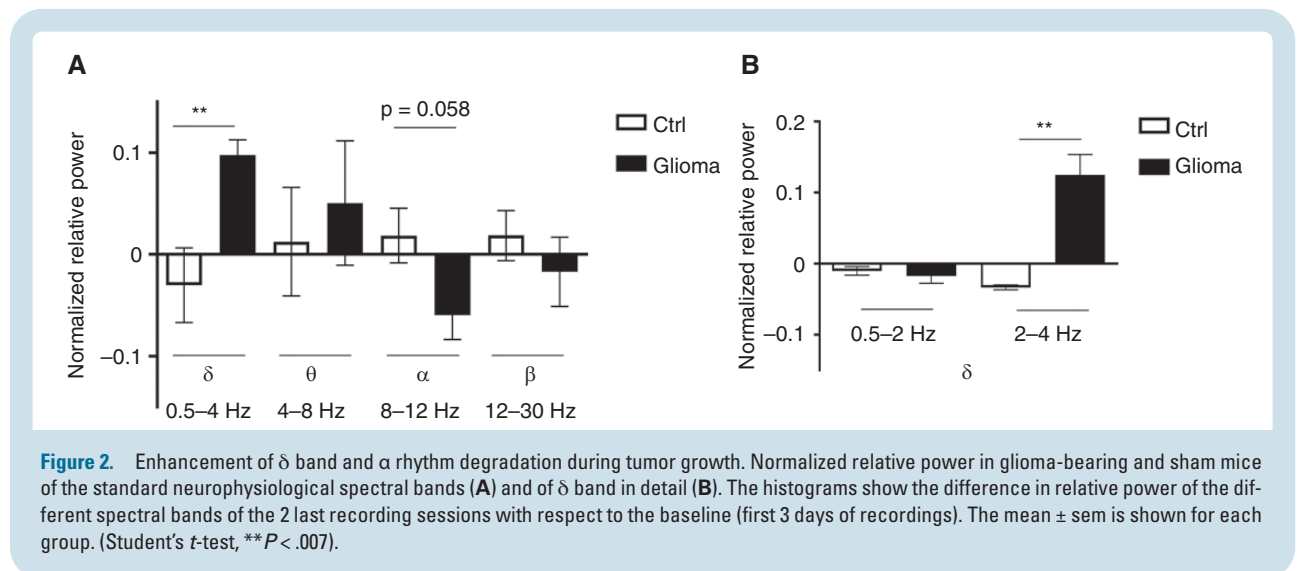
Statistical Analysis

Data shown are mean \pm sem Student's *t*-test or Two-way ANOVA with appropriate post hoc tests were used as detailed. Statistical analyses were conducted using GraphPad Prism 6 software (USA).

Results

Progressive Decay of Visual Response During Tumor Progression

We monitored the cortical activity of the visual cortex along with glioma progression (Figure 1A) and observed that glioma-bearing animals showed a decreased visual responsiveness to both alternating gratings and flash



stimuli (Figure 1D and E) with respect to control mice. During each recording session, the amplitude and the latency of the first 2 main components of VEP (ie, N1 and P1 peaks) were analyzed (Figure 1B and C). As a result, we found an initial progressive increase in VEP amplitude called stimulus-dependent response potentiation (SRP) in both experimental groups, likely indicative of the potentiation of thalamo-cortical synapses due to repetitive visual stimulation.²⁶ However, in glioma-bearing mice, this increase was followed by a rapid decay and deterioration of visual responses that started from day 16 after tumor implantation. Twenty-three days after the cell transplant, a strongly dampened response was detected in glioma-bearing mice. On the contrary, control animals showed reliable VEP responsivity in all the recording sessions (Figure 1D and E). We found no difference between experimental groups in the latency of VEP components, N1 and P1 for both types of visual stimuli (Supplementary Figure 1). This suggests that this parameter is not affected by tumor progression.

Spectral Analysis of LFPs: Enhancement of δ Band During Tumor Growth

To detect whether glioma progression affects ongoing brain oscillations, we analyzed the LFPs recorded during blank stimuli (0% contrast). We focused our attention on the alterations that occurred in the main neurophysiological spectral bands δ , θ , α , and β ²⁷ (Figure 2A). The progression of glioma mass caused a significant increase of the δ band power density with respect to control animals, typical of focal epilepsy,^{28,29} and a trend for α band deterioration. Moreover, we detected changes in the composition of peritumoral slow-wave power (Figure 2B). In particular, glioma-bearing mice showed an increase especially in the “faster” δ band (2-4 Hz) during tumor progression, which might reflect a reduced inhibitory activity in the peritumoral region near the tumor mass.²⁸

Molecular Alterations in Excitatory Peritumoral Neurons

We then analyzed the molecular features of peritumoral neural tissues. After the monitoring of visual cortex activity through VEP analysis, animals were sacrificed, brains were cut and processed for laser-capture microdissection (LCM) to investigate specific gene-expression alterations induced by tumor growth in excitatory pyramidal neurons of layer II-III. Layer II-III was selected since it retains significant potential for plasticity even in adulthood.³⁰ For each sample, we first checked the specificity of dissected neurons by analyzing 2 cell-type specific markers included in the panel: vGlut1 (Slc17a7 gene), as marker of excitatory neurons, and vGat (Slc32a1 gene), for inhibitory ones.³¹ Collected neurons highly expressed Slc17a7 gene and, at the same time, a negligible expression of Slc32a1 was detected (Figure 3C). This result clearly indicated that collected cells were mainly excitatory neurons. Then, the layer specificity of the LCM was checked by analyzing the expression of specific cortical layer markers (Figure 3D and

E). The dissected neurons showed a high expression of Cux1, expressed in layers II-III, with respect to the markers of the deeper layers, confirming the layer specificity of the LCM (Figure 3E).

Among all genes (Figure 4A), 2 targets were significantly altered during glioma progression: The Gabra1 gene, encoding for the GABA-A receptor subunit α 1, and the gene encoding for the pre-synaptic protein SNAP25. Both genes appeared down-regulated in peritumoral excitatory neurons of layers II-III in glioma-bearing mice (Figure 4B). It is worth noticing that, whether the 2-way repeated measure ANOVA found a significant difference among gene expression ($P < .001$, $F = 4.998$), post hoc analysis (with Bonferroni multiple-comparison correction) revealed a statistically significant difference between groups only within the expression of Snap25 ($P = .003$, $F = 24.41$). Although Gabra1 expression indicates only a tendency for downregulation in glioma animals, immunofluorescence experiments in the peritumoral tissue clearly confirmed the reduction of both SNAP25 and GABA-A receptor subunit α 1 proteins (Figure 4C and E).

Interference With GABA-A Receptor Signaling Precipitates Seizures in Both GL261 and CT-2A Bearing Animals

The loss of expression of either SNAP25 or GABA-A α 1 has been previously linked to epilepsy as well as to enhanced propensity for evoked seizures.³² We reasoned that interference with these signaling pathways may unmask seizure susceptibility in glioma-bearing mice. Here we focused on the GABA α 1 receptor subunit which offers several possibilities for pharmacological manipulation. LFPs recordings were performed in freely moving mice³³ to measure seizure activity originating from the tumor-adjacent zone. We were unable to detect spontaneous seizure events in GL261. Next, we employed methyl-6,7-dimethoxy-4-ethyl-beta-carboline-3-carboxylate (DMCM), an inverse benzodiazepine agonist that inhibits GABA currents by binding to the α subunits of the GABA-A receptor. We used a subconvulsant dose of DMCM (1.5 mg/kg; Volke et al., 2003) that we have characterized previously.³⁴ DMCM or vehicle were given i.p. at a late stage of the disease (ie, day 23) in GL261 animals, when changes in GABA α 1 receptor expression are apparent. We found that GL261-bearing animals developed seizures 10'-30' after DMCM administration, whereas control mice did not display any alterations of the LFP recordings after the drug administration (Figure 5A-D). As expected, no changes in excitability were found after saline administration in both experimental groups (Figure 5C and D).

These results were further implemented and confirmed adopting also the CT-2A glioma model, known to be more invasive than the GL261. Thus, in CT-2A-bearing mice we longitudinally monitored hyperexcitability by using electrophysiology and behavioral observations (Figure 6A). The electrophysiological assays here adopted were aimed at evaluating the number of trains (Figure 6B) and seizures (Figure 6C) before and after saline or DMCM. Strikingly, we found that DMCM injection significantly augments the number of trains and seizures in CT-2A animals. In

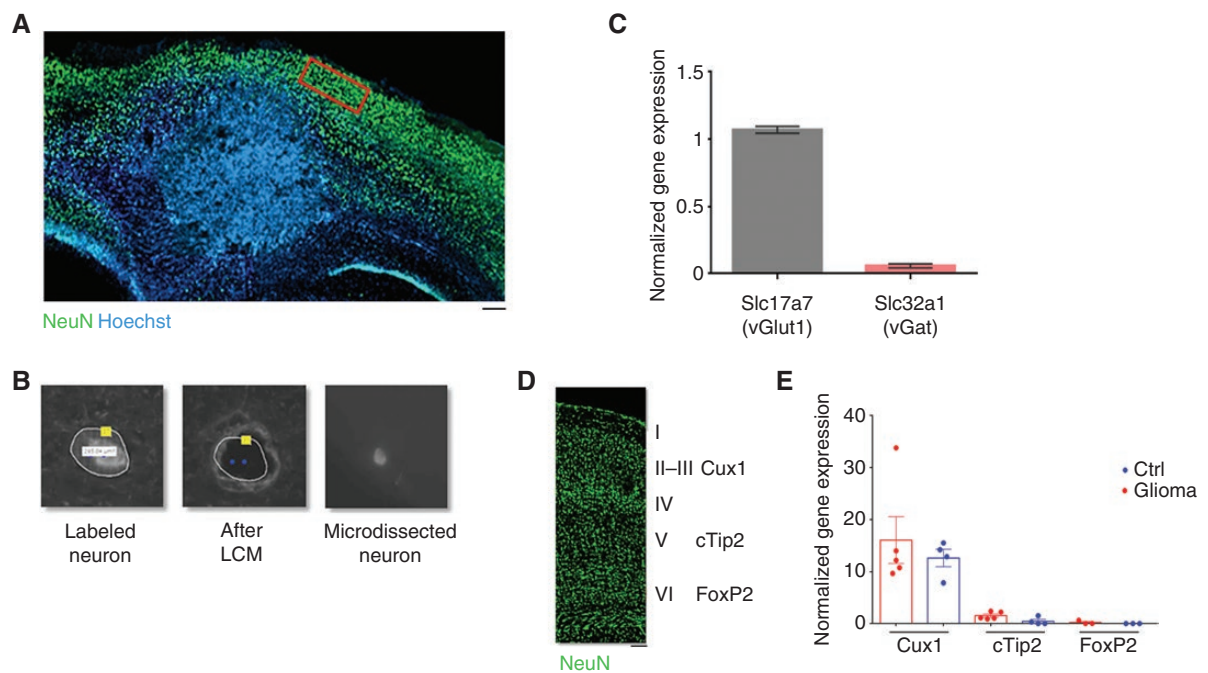


Figure 3. Layer specificity of microdissected neurons. **(A)** Representative tumor mass and peritumoral neurons in the primary visual cortex. The box indicates the ROI for the laser-capture microdissection (LCM). Scale bar, 100 μ m. **(B)** Representative images of LCM: Labeled neurons were selected (left), removed by the laser (middle), and collected in the adhesive cap (right). **(C)** Gene-expression analysis of Slc17a7 and Slc32a1 in all samples detected by quantitative real-time PCR. Slc17a7 encoded for vGlut1 protein, specific for glutamatergic neurons; Slc32a1 encoded for the protein vGat specific for inhibitory neurons. The mean \pm sem is shown for each group. **(D)** Layer organization of primary visual cortex and corresponding layer-specific genes included in the panel: Cux1 is a marker of the layers II-III, cTip2 of the layers V-VI, and FoxP2 of the inner layer VI. Scale bar 100 μ m. Gene-expression values were normalized for reference genes and expressed as an increase or decrease relative to the inter-run calibrator (Hellemans et al., 2008; Rieu and Powers, 2009). The mean \pm sem is shown for each group.

parallel, using the Racine scale,^{35,36} we evaluated the presence of behavioral and/or tonic-clonic seizures and, consistently, we observed that, in comparison with controls, CT-2A-bearing mice showed a more epileptic phenotype that worsen after DMCM injection (Figure 6C). To evaluate the level of GABA- α 1 and SNAP25 protein expression between the CT-2A and GL261 model, we performed immunohistochemistry experiments using the same procedure adopted before. Consistently, we found a strong reduction in the level of those 2 markers (Figure 6D). Altogether, these data prove that: (1) in both models, GL261 and CT-2A, an acute downregulation of GABA-A receptor signaling precipitates seizures, and (2) common molecular alterations are present in both GL261 and CT-2A mouse models and that, modulating GABA-A signaling, those glioma mice are more susceptible to developing seizures.

Discussion

The results described in this paper aim to provide novel evidence on the complex scenario of neuron-glioma interactions. Through longitudinal recordings of visually evoked potentials, we monitored glioma-induced neural dysfunctions in control animals and mice bearing gliomas in the

occipital cortex. We detected a dampening of the amplitude but not of the latency of visual responsivity in glioma-bearing animals along with tumor progression (Figure 1, Supplementary Figure 1). Moreover, in the same area, we recorded abnormal brain oscillations (Figure 2), with an enhancement of brain activity in lower frequency bands. The increased slow-wave activity was previously associated with poorer cognitive functions in low-grade glioma patients (working memory, information processing, and executive functioning;³⁷). These glioma-driven changes in spectral bands could be linked to the disruption of functional connectivity with regions connected to the site of the tumor,³⁷ as reported in MRI studies in humans.³⁸ Increased delta waves have been previously shown in different focal brain lesions and in a variety of neural disorders characterized by altered functional connectivity,³⁹ such as focal epilepsy.^{28,40} The increase in the δ band is mainly determined by the enhancement of 2-4 Hz oscillations, a hallmark shared with focal epilepsy patients²⁸ (Figure 2).

Overall, our data suggest that electrophysiological parameters such as sensory-driven responses and EEG spectral power may be used for the monitoring of glioma subjects, with a potential prognostic value.

Damages at the level of tissue and neural connectivity could cause an imbalance between inhibition and excitation, mechanism that plays a pivotal role in tumor-associated epilepsy in patients. These epileptogenic

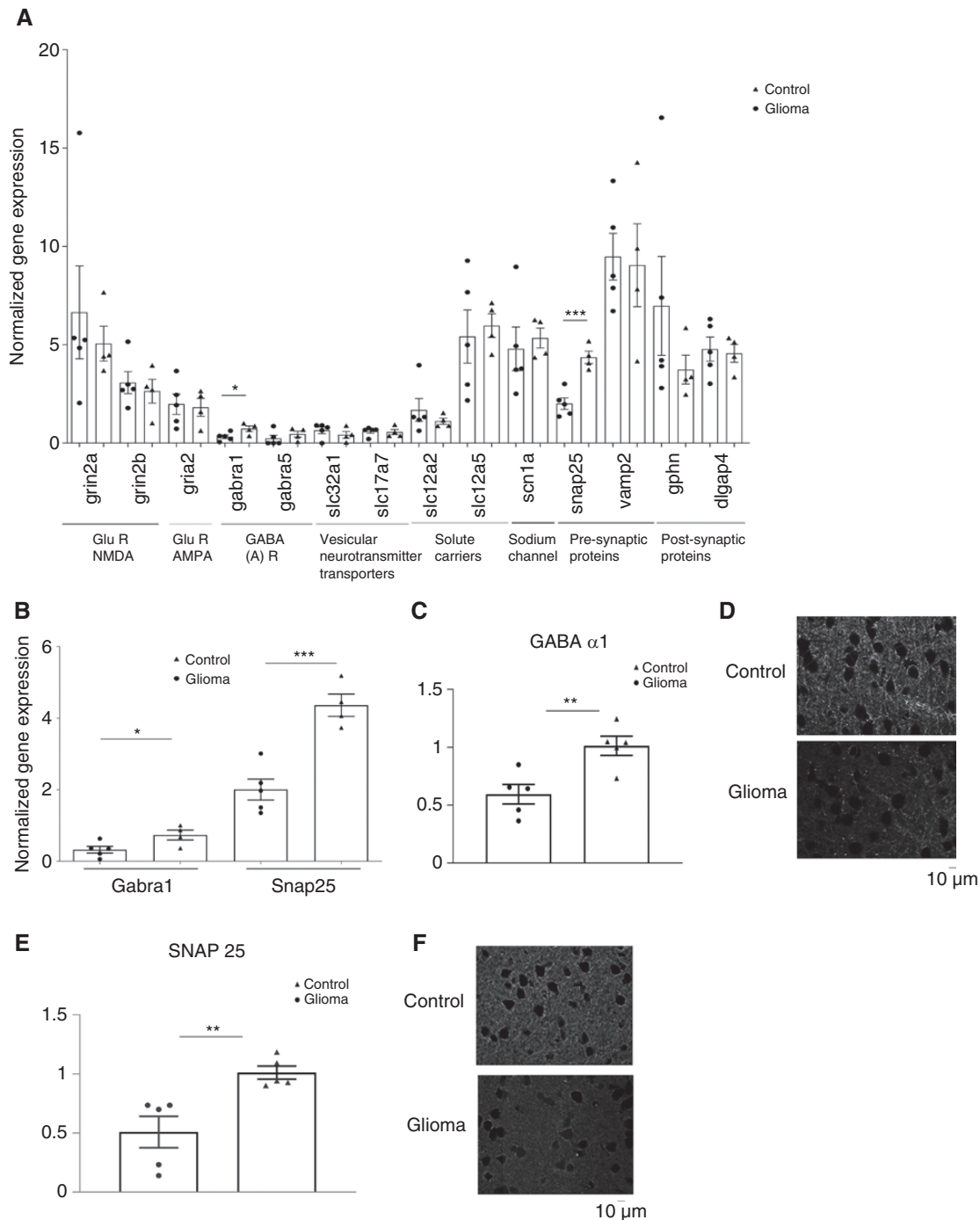


Figure 4. Pre- and post-synaptic alterations in peritumoral excitatory neurons. (A) Expression analysis of a customized panel of genes detected by quantitative real-time PCR in dissected neurons from glioma-bearing (Glioma) and control (Ctrl) mice. The colored bars under the histogram represent a classification of genes: red= Glu R NMDA (Glutamate NMDA receptor subunit), yellow= Glu R AMPA (Glutamate AMPA receptor subunit), green= GABA-A R (GABA-A receptor subunit), cyan= Vesicular neurotransmitter transporters, blue= sodium channel, pink= pre-synaptic proteins, orange= post-synaptic proteins. The mean \pm sem is shown. (B) Magnification of genes with a significant alteration in the expression. Gene-expression values were normalized on housekeeping GAPDH and β -actin mRNA and expressed as an increase or decrease relative to the calibrator. The mean \pm sem is also shown (Student's *t*-test, **P* < .05, ****P* < .001). (C, E) Immunofluorescence quantification of GABA-A receptor subunit α 1 and SNAP25 proteins in control (blue) and glioma-bearing (red) mice. Values are normalized with respect to control. The mean \pm sem is shown. (D, F) Representative images of immunofluorescence for GABA-A receptor subunit α 1 and SNAP25 protein in control and Glioma-bearing mice.

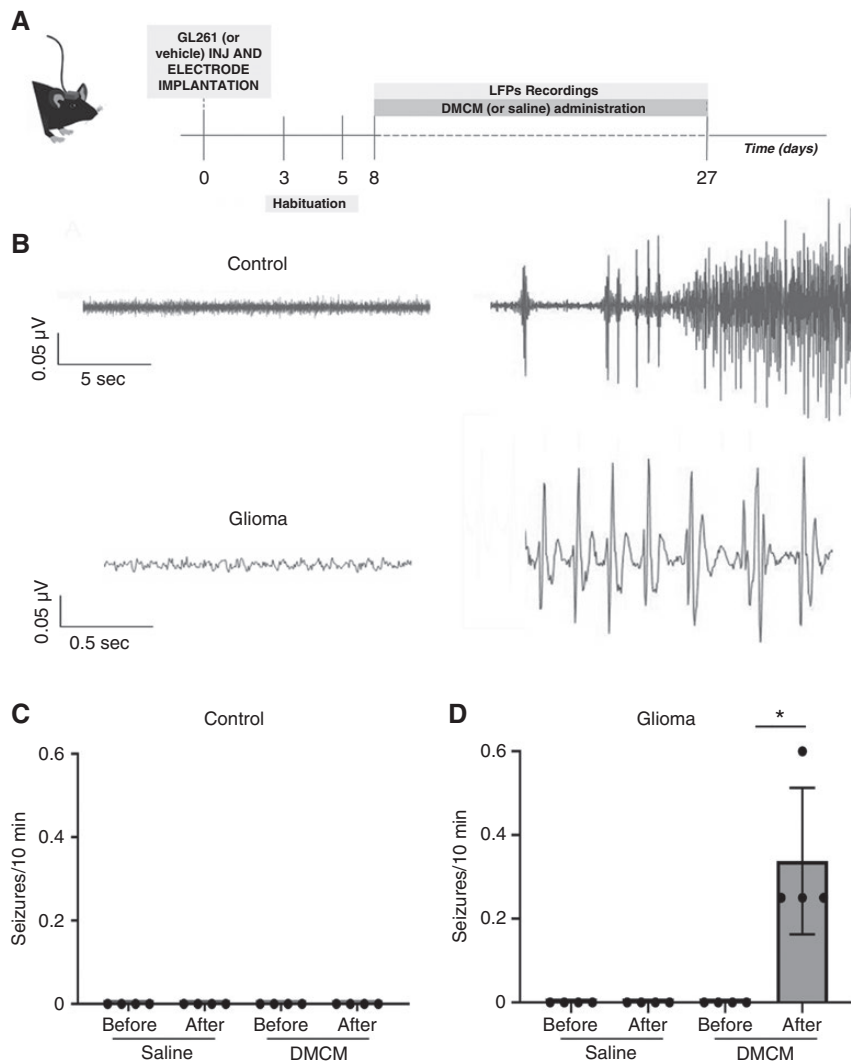


Figure 5. GL261-bearing mice develop seizures at a late stage of the disease after hampering GABA-A receptor signaling. **(A)** On the left is representative image of a mouse implanted with chronic electrodes to record local field potentials (LFPs). On the right is experimental protocol. **(B)** Representative LFP recordings in controls (left) and glioma-bearing (right) mice after DMCM administration. Traces at the bottom show activity on an enlarged scale to better appreciate seizure events. **(C, D)** Frequency of seizure in control **(C)** and glioma-bearing mice **(D)** before and after saline or DMCM administration. The mean \pm sem is also shown (*, $P < .05$).

mechanisms together with molecular features of peritumoral neurons are essential in determining the onset of seizures.⁴¹ We then examined molecular changes in excitatory neurons which accompany their altered physiological responses. Since the activity of pyramidal neurons affects tumor progression,^{13,15,41–43} it is important to identify changes in specific pathways which may be suggested as novel therapeutic targets. We analyzed the expression of a specific panel of genes (Supplementary Table 1) in layer II-III pyramidal neurons, which retain synaptic plasticity throughout adulthood.⁴⁴ They were collected through LCM within the peritumoral region affected by glioma²⁴ and compared with healthy neurons recovered from the primary visual cortex of control animals (Figure 3). Among all the analyzed genes, we found a significant decrease in expression for SNAP25

and GABRA1, which respectively encode for the protein SNAP25 of the SNARE complex and the GABA-A receptor subunit $\alpha 1$, the main inhibitory subunit in the visual cortex,⁴⁵ suggesting an impaired communication between pre- and post-synaptic neurons (Figure 3). These data were confirmed by immunohistochemical analyses performed in the peritumoral tissue of control and glioma mice of 2 different murine glioma models (Figures 4 and 6). The downregulation of SNAP25 could be implicated in the establishment of a pro-epileptic phenotype, as confirmed by SNAP25 heterozygous (SNAP25^{+/-}) mice³² and human epileptic patients.⁴⁶

Despite the well-known role of GABA in epilepsy and in tumor-associated epilepsy,^{9,41,47,48} we here identified a specific downregulation of GABA α 1 receptor subunit that, in animal models, reduces inhibitory drive onto

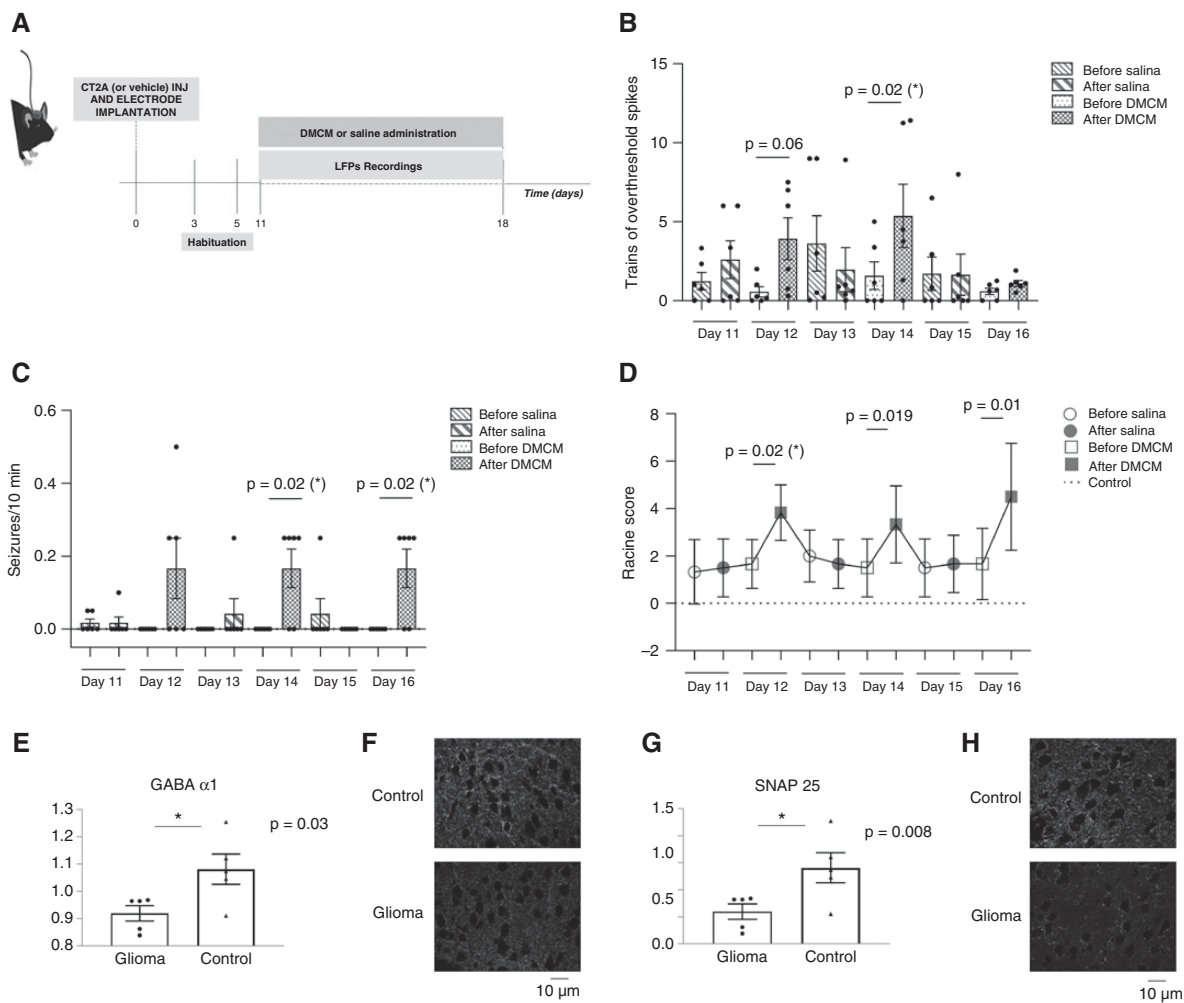


Figure 6. CT-2A-bearing mice showed hallmarks of hyperexcitability at an early stage of the glioma progression and are more prone to develop seizures after hampering GABA-A receptor signaling. **(A)** Experimental protocol used. **(B)** Number of trains in CT-2A animals before and after saline or DMCM administration from day 11 to day 18 after tumor induction. **(C)** Number of seizures in CT-2A animals before and after saline or DMCM administration from day 11 to day 18 after tumor induction. **(D)** Racine scale in CT-2A animals before and after saline or DMCM administration from day 11 to day 18 after tumor induction. The mean \pm sem is shown (*, $P < .05$). **(E, G)** Immunofluorescence quantification of GABA-A receptor subunit $\alpha 1$ and SNAP25 proteins in control (blue) and glioma-bearing (red) mice. Values are normalized with respect to control. The mean \pm sem is shown (*, $P < .05$; **, $P < .01$). **(D, F)** Representative images of immunofluorescence for GABA-A receptor subunit $\alpha 1$ and SNAP25 protein in control and CT-2A-bearing mice.

excitatory circuits, which thus increases their firing rate. As indicated by patch-clamp experiments, peritumoral excitatory neurons of layer II/III show a lowered excitability threshold⁷ and a significant decrement of spontaneous inhibitory synaptic transmission.⁸ A variety of epileptic syndromes have been linked to genetic mutations of GABA-A receptors, including $\alpha 1$.⁴⁹ Moreover, the reduction of GABAergic neural density around tumor mass could concur in a further dysregulation of excitation.⁴⁷ Thus, downregulation of GABA $\alpha 1$ could represent a key event in the cascade of impairments that lead to the imbalance between excitatory and inhibitory networks caused by glioma growth.

To functionally prove the involvement of GABA-A receptor in susceptibility to seizures, we longitudinally recorded LFPs from the tumor-adjacent zone in freely

moving mice in 2 different GBM animal models (ie, GL261 and CT-2A). In GL261 model, we were unable to detect spontaneous seizures during glioma growth in the visual cortex. This may be ascribed to at least a couple of factors: GL261 gliomas typically grow as a large solid mass with limited infiltration into the surrounding tissue, which likely reduces epileptogenicity (Supplementary Figure 2). Second, we employed short periods of recording (1-2 hours daily), and therefore seizures, if infrequent, may be missed. Based on these premises, we attempted to trigger ictal events by further reducing GABA-A receptor signaling with a sub-convulsive dose of DMCM,^{25,34} a benzodiazepine inverse agonist (Figure 5). The reduction of GABA currents by the drug induces epileptiform events only in GL261-bearing mice at a very late stage of the disease (ie, day 27 after

tumor induction), suggesting that peritumoral tissues are more prone to provoke seizures.

We then tested DMCM administration on a more infiltrative and aggressive murine model, created by the injection of CT-2A cells in the visual cortex. In line with the more infiltrative features of this model (Supplementary Figure 2), CT-2A mice showed hallmarks of hyperexcitability in the visual cortex at an early stage of the glioma progression (ie, starting from day 11 after tumor induction; Figure 6B and C). Remarkably, in the CT-2A model, we also found that seizures spread from the visual cortex to other parts of the brain, resulting in pre- and convulsive behaviors (Figure 6D). Similarly to the GL261 model, CT-2A hyperexcitability worsen after hampering GABA-A receptor signaling (Figure 6B–D) and the downregulation of both SNAP25 and GABA α 1 proteins were also observed (Figure 6E–H).

Since epilepsy is the most common comorbidity in patients with gliomas and its control is currently unsatisfactory,⁵⁰ our findings are of particular importance because they reveal novel molecular players in pyramidal neurons which may be targeted for preventing neuronal dysfunction and hyperexcitability,^{11,16,43} potentially leading to the development of innovative drugs that might be ameliorating patients' quality of life.

Supplementary Material

Supplementary material is available online at *Neuro-Oncology* (<http://neuro-oncology.oxfordjournals.org/>).

Keywords

glioma | laser capture | mouse model | microdissection | seizure | visual cortex

Funding

This research was funded by Associazione Italiana per la ricerca sul Cancro, [grant numbers IG#18925 and IG#26044], and by Ministero dell'Istruzione e del Merito, Progetti di Rilevante Interesse Nazionale projects [20178L7WRS and 2020Z73J5A].

Acknowledgments

We thank Francesca Biondi for the excellent animal care and Elena Novelli for the technical support with immunohistochemistry analyses. At the time of the experiments, EV and CC were supported by a postdoctoral fellowship released by Fondazione Umberto Veronesi (Milan, Italy).

Conflict of interest statement

None declared.

Authorship statement

Electrophysiology and molecular analyses: E.T.; electrophysiology: E.V. and C.C.; immunostaining: M.S. and E.D.S.; electrophysiological data analysis: N.M. and A.M.; laser-capture microdissection: M.M. and C.M.M.; supervision of the work: M.Ca, M.Co, E.V. Unfortunately, we have to communicate that Prof. Matteo Caleo, last author and designer of this study, tragically passed away during the initial steps of this revision.

Affiliations

CNR Neuroscience Institute, Pisa, Italy (E.T., M.S., E.D.S., M.C., E.V., M.C.); Fondazione Pisana per la Scienza Onlus (FPS) Pisa, Italy (E.T., M.M., C.M.M.); The Biorobotics Institute, Scuola Superiore Sant'Anna, Pisa, Italy (N.M., A.M.); Department of Excellence for Robotics and AI, Scuola Superiore Sant'Anna, Pisa, Italy (N.M., A.M.) Fondazione Umberto Veronesi, Milan, Italy (C.C., E.V.); Department of Pharmacy, University of Pisa, Pisa, Italy (C.C.); Department of Biomedical Sciences, University of Padua, Padua, Italy (M.C.); Centro Pisano ricerca e implementazione clinica Flash Radiotherapy "CPFR@CISUP," "S. Chiara" Hospital, Pisa, Italy (M.C., E.V.); Laboratory of Biology BIO@SNS, Scuola Normale Superiore, Pisa, Italy (M.C.)

References

- van Kessel E, Baumfalk AE, van Zandvoort MJE, Robe PA, Snijders TJ. Tumor-related neurocognitive dysfunction in patients with diffuse glioma: a systematic review of neurocognitive functioning prior to anti-tumor treatment. *J Neurooncol*. 2017;134(1):9–18.
- Rzeski W, Turski L, Ikonomidou C. Glutamate antagonists limit tumor growth. *Proc Natl Acad Sci U S A*. 2001;98(11):6372–6377.
- Sontheimer H. A role for glutamate in growth and invasion of primary brain tumors. *J Neurochem*. 2008;29(1):61–71.
- Vannini E, Olimpico F, Middei S, et al. Electrophysiology of glioma: a Rho GTPase-activating protein reduces tumor growth and spares neuron structure and function. *Neuro Oncol*. 2016;18(12):1634–1643.
- Armstrong TS, Grant R, Gilbert MR, Lee JW, Norden AD. Epilepsy in glioma patients: mechanisms, management, and impact of anticonvulsant therapy. *Neuro Oncol*. 2016;18(6):779–789.
- Cowie CJA, Cunningham MO. Peritumoral epilepsy: relating form and function for surgical success. *Epilepsy Behav*. 2014;38:53–61.
- Buckingham SC, Campbell SL, Haas BR, et al. Glutamate release by primary brain tumors induces epileptic activity. *Nat Med*. 2011;17(10):1269–1274.

8. Campbell SL, Robel S, Cuddapah VA, et al. GABAergic disinhibition and impaired KCC2 cotransporter activity underlie tumor-associated epilepsy. *Glia*. 2015;63(1):23–36.
9. Pallud J, Le Van Quyen M, Bielle F, et al. Cortical GABAergic excitation contributes to epileptic activities around human glioma. *Sci Transl Med*. 2014;6(244):244ra89.
10. Tewari BP, Chaunsali L, Campbell SL, et al. Perineuronal nets decrease membrane capacitance of peritumoral fast spiking interneurons in a model of epilepsy. *Nat Commun*. 2018;9(1).
11. Yu K, Lin CCJ, Hatcher A, et al. PIK3CA variants selectively initiate brain hyperactivity during gliomagenesis. *Nature*. 2020;9(1):4724.
12. Gill BJA, Khan FA, Merricks EM, et al. Single unit analysis and wide-field imaging reveal alterations in excitatory and inhibitory neurons in glioma. *Brain*. 2022;145(10):3666–3680.
13. Venkatesh HS, Morishita W, Geraghty AC, et al. Electrical and synaptic integration of glioma into neural circuits. *Nature*. 2019;573(7775):539–545.
14. Venkataramani V, Tanev DI, Kuner T, Wick W, Winkler F. Synaptic input to brain tumors: clinical implications. *Neuro Oncol*. 2021;23(1):23–33.
15. Wang YH, Huang TL, Chen X, et al. Glioma-derived TSP2 promotes excitatory synapse formation and results in hyperexcitability in the peritumoral cortex of glioma. *J Neuropathol Exp Neurol*. 2021;141:104942.
16. Tantillo E, Vannini E, Cerri C, et al. Differential roles of pyramidal and fast-spiking, GABAergic neurons in the control of glioma cell proliferation. *Neurobiol Dis*. 2020;141:104942.
17. Frenkel MY, Sawtell NB, Diogo ACM, et al. Instructive effect of visual experience in mouse visual cortex. *Neuron*. 2006.
18. Kantz H, Schreiber T. Nonlinear Time Series Analysis. *Chaos*. 2015;25(9):097610.
19. Stine RA, Abarbanel HDI. Analysis of observed chaotic data. *Technometrics*. 1997;39:334–335.
20. Fink L, Kinfe T, Stein MM, et al. Immunostaining and laser-assisted cell picking for mRNA analysis. *Lab Invest*. 2000;80(3):327–333.
21. Fink L, Kwapiszewska G, Wilhelm J, Bohle RM. Laser-microdissection for cell type- and compartment-specific analyses on genomic and proteomic level. *Exp Toxicol Pathol*. 2006;57(Suppl 2):25–29.
22. Buckanovich RJ, Sasaroli D, O'Brien-Jenkins A, et al. Use of immunolocalization to identify the in situ expression profile of cellular constituents of the tumor microenvironment. *Cancer Biol Ther*. 2006;5(6):35–42.
23. Butler AE, Matveyenko AV, Kirakossian D, et al. Recovery of high-quality RNA from laser capture microdissected human and rodent pancreas. *J Histotechnol*. 2016;39(2):59–65.
24. Seano G, Nia HT, Emblem KE, et al. Solid stress in brain tumours causes neuronal loss and neurological dysfunction and can be reversed by lithium. *Nat Biomed Eng*. 2019;3(3):230–245.
25. Volke V, Wegener G, Vasar E. Augmentation of the NO-cGMP cascade induces anxiogenic-like effect in mice. *J Physiol Pharmacol*. 2003;54(4):653–60.
26. Cooke SF, Bear MF. How the mechanisms of long-term synaptic potentiation and depression serve experience-dependent plasticity in primary visual cortex. *Philos Trans R Soc B Biol Sci*. 2014;368(1633):20130284.
27. Buzsáki G. *Rhythms of the Brain*. New York: Oxford Academic; 2009. doi: [10.1093/acprof:oso/9780195301069.001.0001](https://doi.org/10.1093/acprof:oso/9780195301069.001.0001)
28. Lundstrom BN, Boly M, Duckrow R, Zaveri HP, Blumenfeld H. Slowing less than 1 Hz is decreased near the seizure onset zone. *Sci Rep*. 2019;9(1):6218.
29. Schönherr M, Stefan H, Hamer HM, et al. The delta between postoperative seizure freedom and persistence: automatically detected focal slow waves after epilepsy surgery. *Neuroimage Clin*. 2016;13:256–263.
30. La Rosa C, Parolisi R, Bonfanti L. Brain structural plasticity: from adult neurogenesis to immature neurons. *Front Neurosci*. 2020;14:75.
31. Edwards RH. The neurotransmitter cycle and quantal size. *Neuron*. 2007;55(6):835–858.
32. Corradini I, Donzelli A, Antonucci F, et al. Epileptiform activity and cognitive deficits in SNAP-25+/- mice are normalized by antiepileptic drugs. *Cereb Cortex*. 2014;24(2):364–376.
33. Cerri C, Genovesi S, Allegra M, et al. The chemokine CCL2 mediates the seizure-enhancing effects of systemic inflammation. *J Neurosci*. 2016;36(13):3777–3788.
34. Alia C, Spalletti C, Lai S, et al. Reducing GABA A-mediated inhibition improves forelimb motor function after focal cortical stroke in mice. *Sci Rep*. 2016;6(November):1–15.
35. Tripathi PP, Di Giovannantonio LG, Viegi A, et al. Serotonin hyperinnervation abolishes seizure susceptibility in Otx2 conditional mutant mice. *J Neurosci*. 2008;28(37):9271–9276.
36. Van Erum J, Van Dam D, De Deyn PP. PTZ-induced seizures in mice require a revised Racine scale. *Epilepsy Behav*. 2019;95:51–55.
37. Bosma I, Reijneveld JC, Klein M, et al. Disturbed functional brain networks and neurocognitive function in low-grade glioma patients: a graph theoretical analysis of resting-state MEG. *Nonlinear Biomed Phys*. 2009;3(1):1–11.
38. Stoecklein VM, Stoecklein S, Galiè F, et al. Resting-state fMRI detects alterations in whole brain connectivity related to tumor biology in glioma patients. *Neuro Oncol*. 2020.
39. Assenza G, Fioravante C, Lazzaro di B, et al. Oscillatory activities in neurological disorders of elderly: biomarkers to target for neuromodulation. *Front Aging Neurosci*. 2017;22(9):1388–1398.
40. Pellegrino G, Tombini M, Curcio G, et al. Slow activity in focal epilepsy during sleep and wakefulness. *Clin EEG Neurosci*. 2017;9:189.
41. Bruna J, Miró J, Velasco R. Epilepsy in glioblastoma patients: basic mechanisms and current problems in treatment. *Expert Rev Clin Pharmacol*. 2013;48(3):200–208.
42. Venkatesh HS, Johung TB, Caretti V, et al. Neuronal activity promotes glioma growth through neuroligin-3 secretion. *Cell*. 2015;161(4):803–816.
43. Venkataramani V, Tanev DI, Strahle C, et al. Glutamatergic synaptic input to glioma cells drives brain tumour progression. *Nature*. 2019;573(7775):532–538.
44. Maffei A, Turrigiano GG. Multiple modes of network homeostasis in visual cortical layer 2/3. *J Neurosci*. 2008.
45. Fuchs C, Abitbol K, Burden JJ, et al. GABAA receptors can initiate the formation of functional inhibitory GABAergic synapses. *Eur J Neurosci*. 2013;38(8):3146–3158.
46. Rohena L, Neidich J, Truitt Cho M, et al. Mutation in SNAP25 as a novel genetic cause of epilepsy and intellectual disability. *Rare Dis*. 2013;1:e26314.
47. Komiyama K, Iijima K, Kawabata-Iwakawa R, et al. Glioma facilitates the epileptic and tumor-suppressive gene expressions in the surrounding region. *Sci Rep*. 2022;12(1):1–12.
48. MacKenzie G, O'Toole, KK, Moss, JS, Maguire J. Compromised GABAergic inhibition contributes to tumor-associated epilepsy. *Physiol Behav*. 2017;176(1):139–148.
49. Macdonald RL, Kang JQ, Gallagher MJ. Mutations in GABAA receptor subunits associated with genetic epilepsies. *J Physiol*. 2010;588(Pt 11):1861–1869.
50. You G, Zhiyi S, Jiang T. Clinical diagnosis and perioperative management of glioma-related epilepsy. *Front Oncol*. doi: [10.3389/fonc.2020.550353](https://doi.org/10.3389/fonc.2020.550353).